

Proceeding Paper

# Preliminary Studies on the Synthesis of Redox-Labelled Molecularly Imprinted Nanoparticles in Sensor Development for the Quantification of Perfluoroalkyls in Water <sup>†</sup>

Marco Costa <sup>1</sup>, Sabrina Di Masi <sup>1,\*</sup>, Christopher Zaleski <sup>2</sup>, Sergey A. Piletsky <sup>2</sup> and Cosimino Malitesta <sup>1</sup>

<sup>1</sup> Laboratorio di Chimica Analitica, Dipartimento di Scienze e Tecnologie Biologiche ed Ambientali (DiSTeBA), Università del Salento, Via Per Monteroni, 73100 Lecce, Italy; marco.costa@unisalento.it (M.C.); cosimino.malitesta@unisalento.it (C.M.)

<sup>2</sup> Department of Chemistry, University of Leicester, University Rd, Leicester LE1 7RH, UK; cz155@leicester.ac.uk (C.Z.); sp523@leicester.ac.uk (S.A.P.)

\* Correspondence: sabrina.dimasi@unisalento.it

<sup>†</sup> Presented at the 3rd International Electronic Conference on Biosensors, 8–21 May 2023; Available online: <https://iecb2023.sciforum.net/>.

**Abstract:** Polyfluoroalkyl compounds (PFASs) are synthetic compounds recently classified as permanent and emerging chemicals ever since their bioaccumulation in humans and the environment, due to the presence of carbon–fluorine functional groups. The design of novel screening tools with addressed high response time for the routine quantification of PFASs in water is highly desirable. In this work, we propose the preparation of a new voltammetric sensor based on molecularly imprinted polymer nanoparticle (nanoMIP) receptors for the highly sensitive and selective quantification of PFASs in water. The nanoMIPs were synthesized by the solid phase approach and immobilized onto functionalized screen-printed platinum electrode (SPPtE), chosen as the transduction element for sensor development. Dimensional characterization of nanoMIPs by Dynamic light scattering (DLS) shows small nanosized imprinted particles (<200 nm) with a polydispersity index (PDI) below 0.3. Electrochemical techniques were used for sensor preparation, characterization, and to assess the analytical performance, respectively. Preliminary calibration curves of nanoMIP-based sensors in a wide range of PFAS concentrations (1.5–100 ng/mL) exhibited high sensitivity toward its target.

**Keywords:** molecularly imprinted polymer; nanoparticles; solid phase synthesis; perfluorooctanoic acid; screen-printed electrode; voltammetric sensor



**Citation:** Costa, M.; Di Masi, S.; Zaleski, C.; Piletsky, S.A.; Malitesta, C. Preliminary Studies on the Synthesis of Redox-Labelled Molecularly Imprinted Nanoparticles in Sensor Development for the Quantification of Perfluoroalkyls in Water. *Eng. Proc.* **2023**, *35*, 22. <https://doi.org/10.3390/IECB2023-14589>

Academic Editor: Danila Moscone

Published: 9 May 2023



**Copyright:** © 2023 by the authors. Licensee MDPI, Basel, Switzerland. This article is an open access article distributed under the terms and conditions of the Creative Commons Attribution (CC BY) license (<https://creativecommons.org/licenses/by/4.0/>).

## 1. Introduction

Perfluorooctanoic acid (PFOA) belongs to the large class of perfluorinated chemicals (PFCs), synthetic substances that have been produced in industrial processes and for commercial purposes for over 60 years [1]. Their properties, such as oil and water repellency and resistance to heat and chemical reactions, are due to their structure, which includes a fully fluorinated carbon chain that is both hydrophobic and oleophobic, and a hydrophilic charged functional group such as carboxylic acid. For this reason, they are used in water-repellent, stain-resistant coatings for clothing, leather, upholstery, and carpets; in oil-repellent coatings for paper that comes into contact with food; in fire-fighting foams; in paints and other commercial products; and in industries as surfactants, emulsifiers, wetting agents, additives and coatings. PFOA and other PFCs produced mainly by two manufacturing processes (electrochemical fluorination, ECF, and telomerization) [1,2] are in the spotlight as environmental pollutants. Public opinion and concerns about them continue to also grow, thanks to the availability of new and recent studies that provide information on their presence in the environment, fate, and transport, as well as on the effects of human exposure. Their hazardousness is not only due to their effects on our

organism, but also to their persistence, being very resistant to typical environmental degradation processes due to their carbon–fluorine bonds, which are among the strongest in organic chemistry [3]. Their presence has been detected in environmental matrices around the world, including finished drinking water, surface water, groundwater, air, sludge, soil, sediment, indoor dust, biota, and ice caps [4]. The production and use of PFOA are currently being phased out, but environmental contamination and human exposure to PFOA are expected to continue into the foreseeable future because it is persistent and arises from precursor compounds such as the degradation of compounds such as fluorotelomer alcohols (FTOH) used in industries and various products [2,5]. PFOA concentrations ranging from 12.6 ng/L to 287 ng/L were detected by UPLC-MS/MS [6]. Although HPLC/HRMS is still an accurate analytical method that can detect a wide range of analytes, it has practical disadvantages, such as high cost and lack of user experience in handling and interpreting the data, etc. Therefore, portable, sensitive, and highly selective sensors capable of detecting low concentrations of PFOA in real matrices are desirable. Biosensors and chemical sensors offer rapid measurements and responses, easy-to-use platforms, portability, low-cost fabrication, and high sensitivity [7,8]. Molecularly imprinted polymers (MIPs) have been widely used as synthetic receptors in sensor development [9,10] and provide the high sensitivity and selectivity of biological receptors, while their polymeric nature makes them resistant to harsh conditions [11]. The use of MIPs in the form of nanoparticles (nanoMIPs) allows for the production of analyte-compliant cavities, thus possessing higher specificity and overall performance than traditional techniques [12]. The regular distribution of analyte binding sites also leads to efficient mass transfer, which enables rapid detection of the analyte. In addition, nanoMIPs can be easily synthesized and integrated into a variety of transducers, including electrochemical devices. In this work, we present the preparation of a new electrochemical sensor based on nanoMIPs for the quantification of PFOA in water. The nanoMIPs were prepared by solid-phase approach in the presence of a mixture of functional monomers, cross-linker agents, and the target. The electroactivity of the particles is achieved by introducing a redox marker (ferrocene) into the polymer system, which imparts signaling properties [13]. The resulting PFOA-nanoMIP sensor showed good performance, stability, and high performance.

## 2. Materials and Methods

### 2.1. Materials

Materials used included glass beads, 1-Ethyl-3-(3-dimethylaminopropyl)carbodiimide (EDC), N-hydroxysuccinimide (NHS), acetic anhydride, acetonitrile (AcN), acetone, itaconic acid (ITA), 2-Hydroxyethyl methacrylate (HEMA), ferrocenylmethyl methacrylate (FcMMA), Ethylene Glycol Dimethacrylate (EGDMA), Trimethylolpropane trimethacrylate (TRIM), Pentaerythritol tetrakis (3-mercaptopropionate) (PETMP), Benzyl diethyldithiocarbamate, Dimethylformamide (DMF), ethanol (EtOH), 3-aminopropyltriethoxysilane (APTES), phosphate-buffered solution (PBS) tablet, and perfluorooctanoic acid (PFOA).

### 2.2. Apparatus

Polymerization of nanoMIPs was performed using a UV-lamp ( $0.5 \text{ W cm}^{-1}$ ,  $4 \times 15 \text{ W}$ , Philips HB171/A, Hamburg, Germany). For hot wash step, heating jacket linked with variable power supply was used (TENMA, Bench Power Supply, Farnell, UK). Dynamic light scattering (DLS) was employed to measure the hydrodynamic diameter of the particles using a Zetasizer Nano (Malvern Instruments Ltd., Malvern, UK). For these measurements, 100  $\mu\text{L}$  solution of nanoparticles in 800  $\mu\text{L}$  of water at 25 °C was previously sonicated for 1 min using an Ultrasonic bath (Hilsonic Ultrasonic Cleaner, 20–100 kHz, 220 V). The electrochemical measurements were performed using screen-printed platinum electrodes (SPPtE, Dropsens DRP-550) composed of three-electrode configuration on a planar ceramic support ( $3.3 \times 1 \text{ cm}$ ), and they consisted of a platinum disk-shaped working electrode (4 mm diameter), a platinum electrode as counter electrode, and silver electrode as reference electrode purchased from Metrohm, Runcorn, UK. The electrochemical measurements were performed

by using a Potentiostat (PalmSens4, Dordrecht, The Netherlands). PSTrace 5 was the software to control the instrument and data acquisition.

### 2.3. Preparation of NanoMIPs

Procedure for nanoMIPs preparation was adapted from [14]. Briefly, glass beads (30 g) were activated with 1 M NaOH and then silanized in dry toluene to obtain -NH<sub>2</sub>-bearing beads. After, perfluorooctanoic acid (PFOA) was immobilized on silanized glass beads (PFOA-GB), as shown in Figure 1, via EDC/NHS activation mechanism of template. For this step, the solution was composed of 150 mM of EDC, 225 mM of NHS, and 50 mM of analyte. The reaction time was 2 h under stirring, and then the solution was dried under vacuum until a powder was obtained. Next, unreacted primary amino groups were blocked via Acetic anhydrous (1.5 mL) in AcN (58 mL) reaction, under stirring for 30 min. The mixture was washed with dry acetone and dried under vacuum conditions again. The perfluorooctanoic acid-imprinted polymer nanoparticles (PFOA-nanoMIPs) were synthesized by solid phase synthesis using photo-polymerization in the presence of PFOA-GB. The nanoMIPs polymerization mixture comprised the following: FcMMA (0.05 g, 3.5 mmol) as redox marker, Benzyl diethyldithiocarbamate as iniferter (0.150 g, 12.5 mmol), PETMP (0.36 g, 1.5 mmol) as chain-transfer agent, and EGDMA (0.648 g, 65.3 mmol) and TRIM (0.648 g, 38.3 mmol) as cross-linkers. ITA (0.436 g, 67 mmol) and HEMA (0.067 g, 67 mmol) were selected as functional monomers using computational chemistry. All polymerization components were dissolved in 50 mL of acetonitrile. The mixture was vortexed vigorously until complete dissolution, then sonicated and degassed with nitrogen for 30 min. Afterward, the dry beads (powder) were added to a flat bottom wide crystallizing dish by adding the mixture solution. It was shaken until complete incorporation and contact were obtained. To complete the polymerization, the mixture was exposed to UV radiation for 3 min and then stored in the fridge. The charging-temperature elution step (cold and hot wash) was adopted to elute PFOA from the polymeric structure.

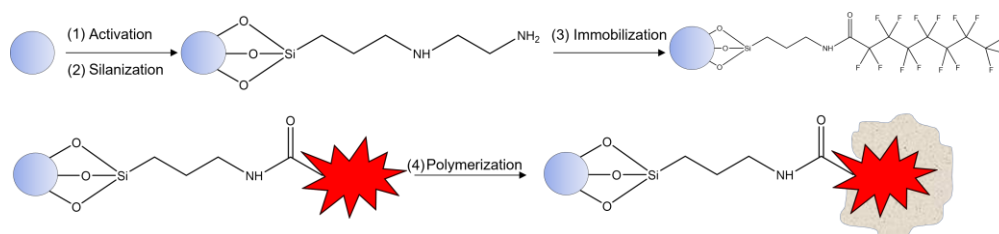


**Figure 1.** General scheme of polymerization protocol.

Prior to the cold wash, nanoMIPs were placed in DMF in the freezer for 1 h, and the glass beads, in powder form, were placed in a syringe. Both ACN and DMF were passed through the syringe for elution of unreacted monomers and low-affinity nanoMIPs. For the hot wash, 100 mL of EtOH was placed in a hot bath (70–80 °C) and was used. At the syringe, warmth was applied by a heating jacket linked with variable power supply. Hot EtOH was passed through into the syringe for elution of high-affinity nanoMIPs. The solution EtOH with nanoMIPs was collected into a round bottom flask, and then the solution was pre-concentrated with rotary evaporation, with the pressure fixed at 175 mbar and the temperature at 60 °C.

### 2.4. Preparation and Electrochemical Characterization of the PFOA-NanoMIP Sensor

Prior to functionalization, the SPpTE was cleaned using ultrapure water. To perform functionalization, 5 µL of 3-aminopropyltriethoxysilane (APTES) solution at a concentration of 5.0% *v/v* (dissolved in ethanol) was dropped on the surface of the working electrode 3 times and then dried at 150 °C for 1 h in an oven. After this procedure, the working electrode was rinsed with ultrapure water to eliminate the excess APTES. Finally, nanoMIPs were immobilized by dropping 100 µL of a solution comprising 20 µL of EDC/NHS (1:1.5)

and 80  $\mu\text{L}$  of nanoMIPs. The incubation time was performed for 40 min. Finally, the developed sensor (PFOA-nanoMIP sensor) was rinsed with water to remove unadsorbed nanoMIPs from the electrode surface. Electrode modification was electrochemically studied using cyclic voltammetry (CV) and differential pulse voltammetry (DPV). Specifically, the electrochemical characterization was performed for bare SPPtE, APTES/SPPtE, and PFOA-nanoMIPs/APTES/SPPtE, respectively, in 5 mM PBS pH 7.2 and in KCl 0.1 M solution including 10 mM ferrocyanide–ferricyanide redox probe.

### 2.5. Characterization of NanoMIPs

The nanoMIP size was evaluated by dynamic light scattering (DLS). DLS is an optical and non-destructive measurement technique for the spectroscopic characterization of dispersed systems. It evaluates high-frequency fluctuation in scattered light. The result of DLS analysis is the intensity-weighted distribution of the particles' hydrodynamic equivalent diameter or hydrodynamic diameter.

### 2.6. PFOA Sensing

The electrochemical performances of the PFOA-nanoMIP sensor towards PFOA were recorded using differential pulse voltammetry (DPV) measurements (in triplicate) in the potential range between  $-0.15\text{ V}$  and  $+0.4\text{ V}$  (vs. Ag reference), with modulation amplitude of  $0.2\text{ V}$ , step potential of  $4.95\text{ mV}$ , equilibration time of  $5\text{ s}$ , and scan rate of  $50\text{ mV/s}$ . Cyclic Voltammetry (CV) was recorded in the potential range from  $-0.1\text{ V}$  to  $+0.8\text{ V}$  (vs. Ag reference), step potential of  $10\text{ mV}$ , and scan rate of  $50\text{ mV/s}$ . The analytical signals of developed sensors were collected by exposure to different increased concentrations of PFOA ( $1.5\text{--}100\text{ ng/mL}$ ) dissolved in phosphate-buffered solution (PBS) ( $5\text{ mM}$ ,  $\text{pH} = 7.4$ ), allowing the specific interaction between the cavities of nanoMIPs and its target. Incubation time was 10 min. After each measurement, the electrode surface was gently washed with ultrapure water.

## 3. Results and Discussions

The polymerization of MIPs based on nanoparticles produced a sensitive receptor for that template, showing high performance and wide margins for improvement. Through the charge given by the FcMMA, it was possible to measure the peak (about  $0.1\text{ V}$ ), whose current intensity decreases with increasing analyte concentration.

### 3.1. Dynamic Light Scattering (DLS) Characterization

Prior to DLS analysis, the prepared nanoMIPs solution was sonicated for 2 min. Subsequently, nanoMIPs were diluted (1:10) in water and analyzed. DLS results displayed a diameter of  $138 \pm 27.80\text{ nm}$  for nanoMIPs, as shown in Figure 2. The polydispersity indexes (PDIs) provide information about the uniformity and mono-dispersive nature of nanoparticles. The PDI of nanoMIPs was 0.137, which indicates a homogeneity and uniform distribution of polymer nanoparticles.

### 3.2. Electrochemical Characterization

The electrochemical characterization for bare SPPtE, APTES/SPPtE, and PFOA-nanoMIPs/APTES/SPPtE is presented in Figure 3, which shows CV and DPV measurements, respectively.

Bare SPPtE exhibited less electrochemical activity in the PBS solution, as expected. After functionalization with APTES, the electrode retained its poor electroactivity. Very interestingly, after PFOA-nanoMIPs immobilization, a reversible redox process was obtained, with oxidation and reduction peaks located at  $+0.21\text{ V}$  and  $-0.195\text{ V}$ , respectively. The aforementioned redox activity is due to the presence of ferrocene-methylmethacrylate moieties in the backbone of nanoMIPs, which was opportunely added during the polymerization stage. The presence of those redox labels can provide a sophisticated and enhanced sensitivity of the receptor towards its target, which is not electroactive at the bare SPPtE. Results were also confirmed by DPV measurements, where a high-peak current at

+0.12 V (now chosen as the electrochemical response of the nanoMIPs) was attributed to the presence of ferrocene, confirming the successful immobilization of PFOA-nanoMIPs.

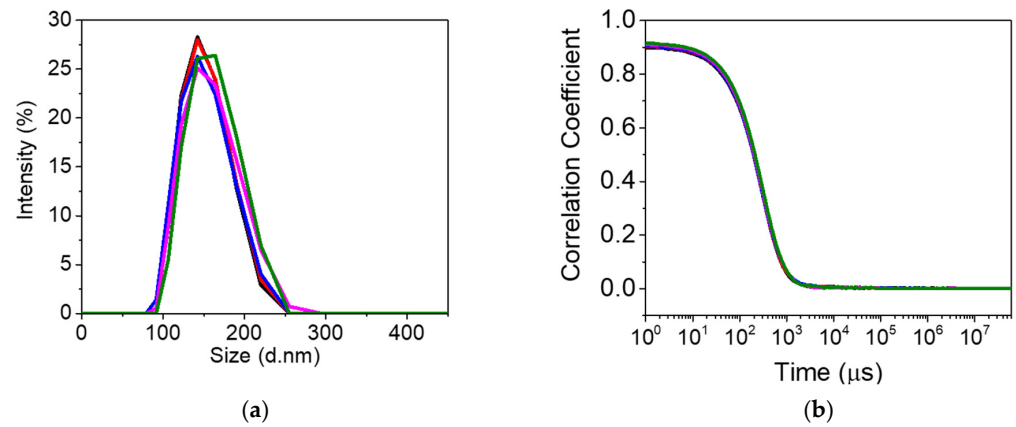


**Figure 2.** Dynamic light scattering analysis ( $n = 5$ ) of the PFOA-nanoMIPs showing (a) particle size distribution and (b) the plot of correlation coefficient vs. time ( $n = 5$ ).

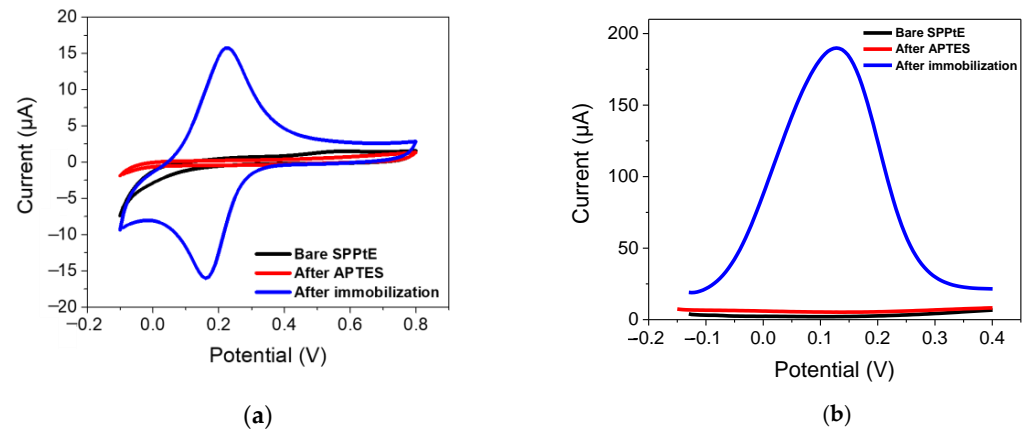


**Figure 3.** Electrochemical characterization by (a) CV (fifth cycle) and (b) DPV in PBS solution for (black) bare screen-printed platinum electrode; (red) functionalized APTES/SPPtE, (blue) after PFOA-nanoMIPs immobilization. DPV condition: (i) Potential range:  $-0.15$  to  $+0.4$  V; (ii) scan rate:  $50 \text{ mV s}^{-1}$ ; (iii) potential step:  $4.95 \text{ mV}$ ; (iv) modulation amplitude:  $0.2 \text{ V}$ ; and (v) time pulse:  $20 \text{ ms}$ . CV condition: (i) potential range:  $-0.1$  to  $+0.8 \text{ V}$ ; (ii) scan rate:  $50 \text{ mV s}^{-1}$ ; and (iii) potential step:  $10 \text{ mV}$ .

### 3.3. Effect of APTES Concentration

To allow maximization of nanoMIP immobilization, the functionalization of SPPtE was investigated. Basically, the effect of APTES concentration ( $0.5, 1, 2.5, 5\% v/v$ ) on the electrochemical response of nanoMIPs was studied by CV and DPV measurement (Figure 4). As visible from DPV measurements in PBS solution, the electrochemical responses of nanoMIPs increase in the intensity peak current by increasing APTES concentration, which can be more accommodating toward the receptor on the electrode surface. For that reason,  $5\%$  of APTES was chosen as the optimum condition for electrode functionalization.

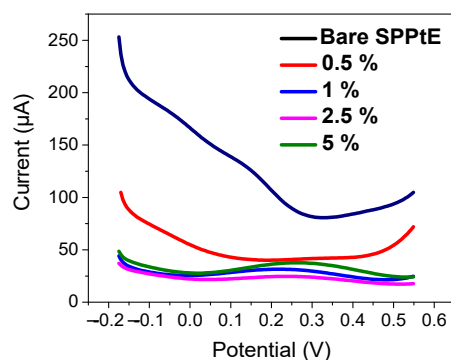


**Figure 4.** Electrochemical characterization by DPV in PBS solution for (black) bare screen-printed platinum electrode; (pink) 0.5%, (blue) 1%, (green) 2.5%, and (purple) 5% of APTES in EtOH *v/v*. DPV condition: (i) potential range:  $-0.175$  to  $+0.6$  V; (ii) scan rate:  $50 \text{ mV s}^{-1}$ ; (iii) potential step:  $4.95 \text{ mV}$ ; (iv) modulation amplitude:  $0.2 \text{ V}$ ; and (v) time pulse:  $20 \text{ ms}$ . CV condition: (i) potential range:  $-0.1$  to  $+0.8 \text{ V}$ ; (ii) scan rate:  $50 \text{ mV s}^{-1}$ ; and (iii) potential step:  $10 \text{ mV}$ .

### 3.4. Analytical Assessment of PFOA-NanoMIP Sensor

The electrochemical sensing of PFOA with the developed PFOA-nanoMIP sensor was investigated by DPV and CV measurements, respectively. The sensor was exposed to distinct PFOA concentrations ranging between  $1.5$  and  $100 \text{ ng/mL}$  in PBS solution (Figure 5).

As shown in Figure 5a, the electroactivity of nanoMIPs greatly decreased with increasing concentration of PFOA. The latter was most visible by DPV measurements (Figure 5b), which can be explained as the interaction of PFOA with the selective cavities. The redox properties of ferrocenylmethyl methacrylate give electroactive properties to nanoMIPs, used for electrochemical sensing of non-electroactive molecules. The selective interaction of the electrode modified with nanoMIPs with the non-electroactive target molecule causes a decrease in the redox current of the ferrocene groups, proportional to the PFOA concentration. This can be attributed to the effect of the non-electroactive analyte on the redox processes of ferrocene. The attenuation of the PFOA binding current results in a restriction of the counterions that access the anchored redox probe to balance the charge, thus hindering the transfer of electrons [15]. In particular, the platform was very sensitive toward PFOA, with a slope of  $0.578 \text{ } \mu\text{A}/\text{ng mL}^{-1}$  and a linear working range between  $0$  and  $6 \text{ ng mL}^{-1}$ . The limit of detection, LOD, calculated as  $3s/m$  where  $s$  was the standard deviation of the intercept and  $m$  is the slope of the regression plot, was  $0.84 \text{ ng mL}^{-1}$ . Saturation of cavities was reached at  $50 \text{ ng/mL}$ , due to the occupancy of cavities. In these cases, the optimal mathematical model, which introduces the nonlinearity, is the sigmoidal model; therefore, the curve fitting was performed using the saturation link of the nonlinear Hill function equation [16] (Figure 5c). The proposed sensor shows high sensitivity and affinity with the analyte. These preliminary results currently encourage us to conduct further experiments with respect to lower concentrations, selectivity properties, and application to real water samples, which we will report shortly.

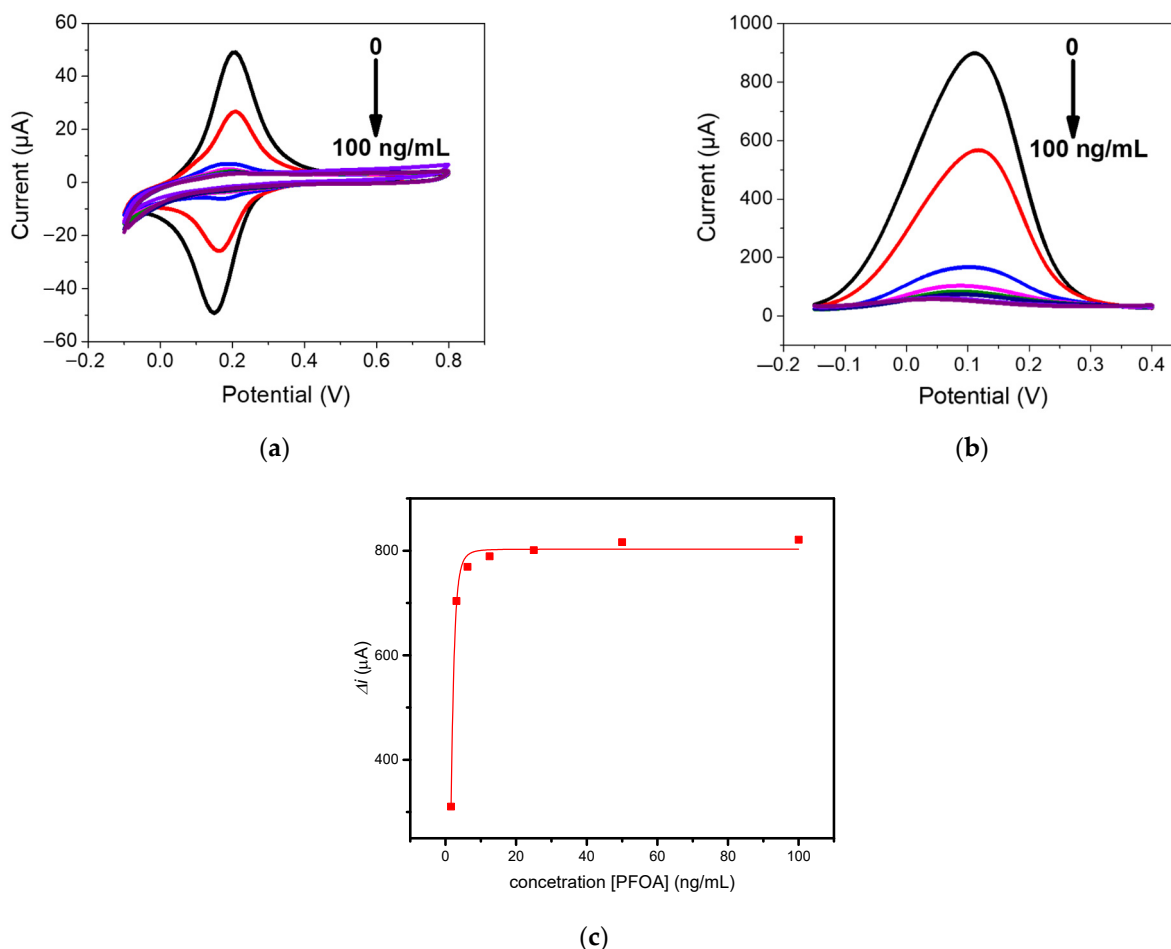


**Figure 5.** (a) CV and (b) DPV measurements performed for PFOA-nanoMIP sensor after exposure to (blank, 0) 1.5, 3, 6, 12, 25, 50, and 100 ng/mL of PFOA dissolved in 5 mM PBS. DPV condition: (i) potential range:  $-0.15$  to  $+0.4$  V; (ii) scan rate:  $50$   $\text{mV s}^{-1}$ ; (iii) potential step:  $4.95$  mV; (iv) modulation amplitude:  $0.2$  V; and (v) time pulse:  $20$  ms. CV condition: (i) potential range:  $-0.1$  to  $+0.8$  V; (ii) scan rate:  $50$   $\text{mV s}^{-1}$ ; and (iii) potential step:  $10$  mV. (c) Related calibration curve fitted with Hill isotherm of PFOA-nanoMIP sensor.

#### 4. Conclusions

Preliminary results on the preparation of a voltammetric sensor based on nanoMIPs for PFOA determination in water were reported. Preparation of nanoMIPs by solid-phase approach in the presence of redox label, such as ferrocenylmethyl methacrylate, provided highly sensitive electroactive receptors for further advanced uses in sensing purposes. The developed platform was assessed towards increased concentration of PFOA in a standard solution of PBS, exhibiting highly sensitive properties. Further experiments to evaluate more properties of the sensor are currently under study.

**Author Contributions:** Conceptualization, S.D.M., C.Z., C.M. and S.A.P.; methodology, M.C. and C.Z.; formal analysis, M.C.; investigation, S.D.M., M.C., C.Z., C.M. and S.A.P.; data curation, M.C. and S.D.M.; writing—original draft preparation, M.C.; writing—review and editing, S.D.M., C.Z., C.M. and S.A.P.; supervision, S.D.M., C.Z., C.M. and S.A.P. All authors have read and agreed to the published version of the manuscript.

**Funding:** This research was funded by the Ph.D. program entitled “Green Analytical Chemistry: development of molecularly imprinted polymers for emerging pollutants” (CUP:F85F21005750001) of “Dottorati su tematiche Green del PON R&I 2014–2020”.

**Institutional Review Board Statement:** Not applicable.

**Informed Consent Statement:** Not applicable.

**Data Availability Statement:** Data will be available upon request.

**Acknowledgments:** The authors would like to thank Alvaro Garcia Cruz for his experimental support.

**Conflicts of Interest:** The authors declare no conflict of interest.

## References

1. Lindstrom, A.B.; Strynar, M.J.; Libelo, E.L. Polyfluorinated compounds: Past, present, and future. *Environ. Sci. Technol.* **2011**, *45*, 7954–7961. [[CrossRef](#)] [[PubMed](#)]
2. Buck, R.C.; Franklin, J.; Berger, U.; Conder, J.M.; Cousins, I.T.; De Voogt, P.; Jensen, A.A.; Kannan, K.; Mabury, S.A.; van Leeuwen, S.P. Perfluoroalkyl and polyfluoroalkyl substances in the environment: Terminology, classification, and origins. *Integr. Environ. Assess. Manag.* **2011**, *7*, 513–541. [[CrossRef](#)] [[PubMed](#)]
3. Vaalgamaa, S.; Vähätalo, A.V.; Perkola, N.; Huhtala, S. Photochemical reactivity of perfluorooctanoic acid (PFOA) in conditions representing surface water. *Sci. Total Environ.* **2011**, *409*, 3043–3048. [[CrossRef](#)] [[PubMed](#)]
4. Lau, C.; Anitole, K.; Hodes, C.; Lai, D.; Pfahles-Hutchens, A.; Seed, J. Perfluoroalkyl acids: A review of monitoring and toxicological findings. *Toxicol. Sci.* **2007**, *99*, 366–394. [[CrossRef](#)] [[PubMed](#)]
5. Butt, C.M.; Berger, U.; Bossi, R.; Tomy, G.T. Levels and trends of poly- and perfluorinated compounds in the arctic environment. *Sci. Total Environ.* **2010**, *408*, 2936–2965. [[CrossRef](#)] [[PubMed](#)]
6. Nakayama, S.F.; Strynar, M.J.; Reiner, J.L.; Delinsky, A.D.; Lindstrom, A.B. Determination of perfluorinated compounds in the Upper Mississippi River Basin. *Environ. Sci. Technol.* **2010**, *44*, 103–1109. [[CrossRef](#)] [[PubMed](#)]
7. Dincer, C.; Bruch, R.; Costa-Rama, E.; Fernández-Abedul, M.T.; Merkoçi, A.; Manz, A.; Urban, G.A.; Güder, F. Disposable sensors in diagnostics, food, and environmental monitoring. *Adv. Mater.* **2019**, *31*, 1806739. [[CrossRef](#)] [[PubMed](#)]
8. Naresh, V.; Lee, N. A review on biosensors and recent development of nanostructured materials-enabled biosensors. *Sensors* **2021**, *21*, 1109. [[CrossRef](#)] [[PubMed](#)]
9. Xiong-Hui, M.A.; Jian-Ping, L.L.; Chao, W.A.N.G.; Guo-Bao, X.U. A review on bio-macromolecular imprinted sensors and their applications. *Chin. J. Anal. Chem.* **2016**, *44*, 152–159.
10. Kadhem, A.J.; Gentile, G.J.; Fidalgo de Cortalezzi, M.M. Molecularly Imprinted Polymers (MIPs) in Sensors for Environmental and Biomedical Applications: A Review. *Molecules* **2021**, *26*, 6233. [[CrossRef](#)] [[PubMed](#)]
11. Ahmad, O.S.; Bedwell, T.S.; Esen, C.; Garcia-Cruz, A.; Piletsky, S.A. Molecularly imprinted polymers in electrochemical and optical sensors. *Trends Biotechnol.* **2019**, *37*, 294–309. [[CrossRef](#)] [[PubMed](#)]
12. Haq, I.; Alanazi, K.; Czulak, J.; Di Masi, S.; Piletska, E.; Mujahid, A.; Hussain, T.; Piletsky, S.A.; Garcia-Cruz, A. Determination of sitagliptin in human plasma using a smart electrochemical sensor based on electroactive molecularly imprinted nanoparticles. *Nanoscale Adv.* **2021**, *3*, 4276–4285. [[CrossRef](#)] [[PubMed](#)]
13. Garcia-Cruz, A.; Ahmad, O.S.; Alanazi, K.; Piletska, E.; Piletsky, S.A. Generic sensor platform based on electro-responsive molecularly imprinted polymer nanoparticles (e-NanoMIPs). *Microsyst. Nanoeng.* **2020**, *6*, 83. [[CrossRef](#)] [[PubMed](#)]
14. Canfarotta, F.; Poma, A.; Guerreiro, A.; Piletsky, S. Solid-phase synthesis of molecularly imprinted nanoparticles. *Nat. Protoc.* **2016**, *11*, 443–455. [[CrossRef](#)] [[PubMed](#)]
15. Khor, S.M.; Liu, G.; Fairman, C.; Iyengar, S.G.; Gooding, J.J. The importance of interfacial design for the sensitivity of a label-free electrochemical immuno-biosensor for small organic molecules. *Biosens. Bioelectron.* **2011**, *26*, 2038–2044. [[CrossRef](#)] [[PubMed](#)]
16. Ko, S.; Gunasekaran, S. Analysis of cheese melt profile using inverse-Hill function. *J. Food Eng.* **2008**, *87*, 266–273. [[CrossRef](#)]

**Disclaimer/Publisher's Note:** The statements, opinions and data contained in all publications are solely those of the individual author(s) and contributor(s) and not of MDPI and/or the editor(s). MDPI and/or the editor(s) disclaim responsibility for any injury to people or property resulting from any ideas, methods, instructions or products referred to in the content.